Negative Ion Photoelectron Spectroscopy Reveals Thermodynamic Advantage of Organic Acids in Facilitating Formation of Bisulfate Ion Clusters: Atmospheric Implications

Gao-Lei Hou,[†,‡,∥] Wei Lin,[§] S. H. M. Deng,[‡] Jian Zhang,[‡,∥] Wei-Jun Zheng,[†] Francesco Paesani,[§] and Xue-Bin Wang*,[‡]

[†]Beijing National Laboratory for Molecular Sciences, State Key Laboratory of Molecular Reaction Dynamics, Institute of Chemistry, Chinese Academy of Sciences, Beijing 100190, China

[‡]Chemical & Materials Sciences Division, Pacific Northwest National Laboratory, P.O. Box 999, MS K8-88, Richland, Washington 99352, United States

[§]Department of Chemistry and Biochemistry, University of California, San Diego, La Jolla, California 92093, United States

Ⓢ *Supporting Information*

ABSTRACT: Recent lab and field measurements have indicated critical roles of organic acids in enhancing new atmospheric aerosol formation. Such findings have stimulated theoretical studies with the aim of understanding the interaction of organic acids with common aerosol nucleation precursors like bisulfate (HSO_4^-). We report a combined negative ion photoelectron spectroscopic and theoretical investigation of molecular clusters formed by HSO_4^- with succinic acid (SUA, $HO_2C(CH_2)_2CO_2H$), $HSO_4^-(SUA)_n$ ($n = 0-2$), along with $HSO_4^-(H_2O)_n$ and $HSO_4^-(H_2SO_4)_n$. It is found that one SUA molecule can stabilize HSO_4^- by ca. 39 kcal/mol, three times the corresponding value that one water molecule is capable of (ca. 13 kcal/mol). Molecular dynamics simulations and quantum chemical calculations reveal the most plausible structures of these clusters and attribute the stability of these clusters to the formation of strong hydrogen bonds. This work provides direct experimental evidence showing significant thermodynamic advantage by involving organic acid molecules to promote formation and growth in bisulfate clusters and aerosols.

SECTION: Environmental and Atmospheric Chemistry, Aerosol Processes, Geochemistry, and Astrochemistry
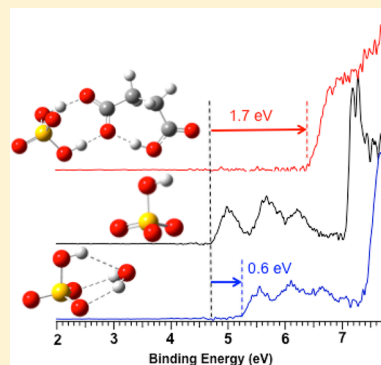
Atmospheric aerosols have received intense research attention over the last several decades as their importance in influencing climate change[1−3] and human health[4−7] has been gradually recognized. Aerosol formation and growth often begin with homogeneous nucleation, in which the first step involves two (binary) or three (ternary) gaseous species interacting with each other to form stable clusters and complexes to decrease nucleation free energy barriers.[8,9] Field measurements[10] have identified sulfuric acid including bisulfate ion as a key atmospheric nucleation precursor in several nucleation mechanisms, including binary $H_2SO_4-H_2O$,[11] ternary $H_2O-H_2SO_4-NH_3$,[12,13] where NH_3 can also be replaced by amines,[14,15] and ion-mediated nucleation.[16,17] The roles of ions and organics in atmospheric nucleation have attracted researchers' interests recently, especially after atmospheric field measurements have revealed that atmospheric aerosols often contain a considerable amount of organic matter[18−20] and various ambient ions.[16,21,22] In 2004, Zhang and coworkers performed a landmark experiment indicating that nucleation rates of sulfuric acid aerosols can be considerably enhanced by the presence of a trace amount of aromatic acids.[23] This pioneering work has stimulated several

experimental studies aimed at characterizing critical roles of different organic compounds in aerosol formation.[24−28]

Size-selected clusters with tunable compositions provide ideal model systems to probe and untangle often complex intermolecular interactions important to the formation of critical nuclei and nucleation embryos. Atmospherically relevant hydrated bisulfate/sulfuric acid clusters have been investigated using IR action spectroscopy,[29,30] mass spectrometry,[31−34] and quantum chemistry calculations.[35,36] Theoretical computations on several hydrogen-bonded clusters consisting of organic species with atmospheric nucleation precursors have been carried out very recently,[37−42] aimed at providing a molecular-level understanding of the mechanisms that allow organic acids to enhance (often significantly) aerosol formation and growth. One important finding from these calculations is that organic acids can form strong hydrogen bonds with nucleation precursors,[37−42] resulting in significant stabilization in energy and reducing nucleation free energy barriers.[8,43]

We report a low-temperature negative ion photoelectron spectroscopy (PES) study on solvation of HSO_4^- by a common dicarboxylic acid, succinic acid (SUA)[18] ($HO_2C(CH_2)_2CO_2H$), to help understand and experimentally probe the first nucleation step of bisulfate aerosols containing organic acids. Like IR spectroscopy that can directly provide the structural information, PES can determine the stabilization energy of HSO_4^- upon the addition of the acid molecules through measurements of the associated spectral electron binding energy (EBE) increase. In addition, molecular dynamics simulations and ab initio quantum calculations reveal the plausible structures for these clusters and provide the EBEs and association energies to compare with the experimental data. To determine the thermodynamic effects due to organic acids in the initial stage of nucleation, we also carried out PES investigations on $HSO_4^-(H_2O)_{1-2}$ and $HSO_4^-(H_2SO_4)_{1-2}$ (where H_2O and H_2SO_4 are important nucleation species in the atmosphere), and the results are directly compared with those obtained with SUA.

The $HSO_4^-(Sol)_n$ (Sol = SUA, H_2O, and H_2SO_4, $n = 0-2$) clusters were produced in the gas phase via electrospray ionization (ESI) of ~0.4 mM aqueous solutions of $(NBu_4)_2SO_4$/SUA (1:1) or $NaHSO_4$/H_2SO_4 (1:1) diluted three times in CH_3CN. Each cluster of interest was first mass-selected, then characterized by a low-temperature PES. (The detailed description of this instrument was given in a recent publication,[44] and the complete experimental procedures can be found in the Supporting Information.) This ESI-PES combined with gas-phase theoretical calculations has been shown to be a powerful approach to obtain the geometric and electronic structures of clusters involving sulfate ions, water molecules, and various organic acids.[45−48]

Figure 1 presents the 20 K PE spectra of $HSO_4^-(Sol)_{0-2}$ (Sol = SUA, H_2SO_4, and H_2O) at 157 nm (7.867 eV). The 193 nm (6.424 eV) PE spectrum of HSO_4^- has been reported by Wang et al. in 2000,[49] and here its 157 nm spectrum shows two more band features (labeled as B, C). Interestingly, a vibrational progression was clearly resolved for the C band with a frequency of 800 ± 40 cm^{-1}. We assigned this frequency to S−OH stretching mode according to the reported vibrational frequencies of the bisulfate ion,[29,30] which is also confirmed by our theoretical analysis (vide infra). On the basis of the rapidly rising onset energies for all $HSO_4^-(Sol)_1$ species, estimates of the adiabatic electron detachment energies (ADEs) of 4.75 (HSO_4^-), 6.45 (HSO_4^-·SUA), 6.55 (HSO_4^-·H_2SO_4), and 5.35 eV (HSO_4^-·H_2O) were obtained (Table 1) and found to increase from that of bisulfate upon its binding with each solvent molecule as expected because ion molecular interaction is stronger than the interaction between neutral molecules. One most surprising finding is that the addition of one SUA or H_2SO_4 molecule has induced a huge EBE increase of ca. 1.7 to 1.8 eV for $HSO_4^-(SUA)_1$ and $HSO_4^-(H_2SO_4)_1$ from that of HSO_4^-, whereas one H_2O induced only about ca. 0.6 eV EBE increase. These EBE increases correspond to the binding energy differences between HSO_4^- and $HSO_4^·$ with each solvent molecule, reflecting lower limits for the stabilization of the bisulfate anion by one SUA, sulfuric acid, and water molecule, that is, 39.2, 41.5, and 13.8 kcal/mol, respectively. The much larger EBEs of the SUA and sulfuric acid clusters relative to that of water illustrate an enhanced stabilization of the bisulfate anion by these two acids. This is the first direct experimental observation showing the remarkable thermodynamic advantage by involving organic acids in initial nucleation
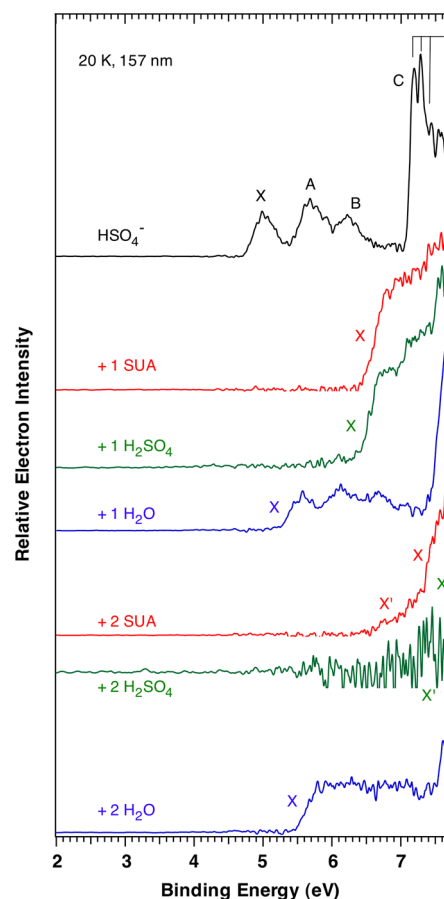

Figure 1. 20 K photoelectron spectra of $HSO_4^-(Sol)_{0-2}$ (Sol = SUA, H_2SO_4, and H_2O) at 157 nm (7.867 eV). The vibrational progression of the C band of HSO_4^- is indicated. X and X' indicate band features coming from different isomers.

steps and also in agreement with the much higher stability of $HSO_4^-(H_2SO_4)_n$ versus $HSO_4^-(H_2O)_n$ found in recent computations and mass spectrometric measurements.[34,50,51]

The PE spectra of $HSO_4^-(Sol)_2$ exhibit further stabilization upon association of the second SUA, H_2SO_4, and H_2O molecules onto the respective monosolvated clusters, that is, 0.15, 0.65, and 0.20 eV EBE increases, respectively, albeit at much smaller paces (Figure 1). There is a very long rising onset for the spectrum of $HSO_4^-(SUA)_2$, indicating either the existence of multiple isomers (X' and X) or large geometric changes upon photodetachment. The signal-to-noise ratio of the PE spectrum of $HSO_4^-(H_2SO_4)_2$ is poor, presumably due to its extremely high EBE considering that it was taken under similar conditions (ion intensity and photon flux) as the other two clusters ($HSO_4^-(H_2O)_2$ and $HSO_4^-(SUA)_2$). Nevertheless, two spectral features at the extremely high EBE side, that is, X' of 7.2 eV and X with EBE >7.5 eV, can be identified in the spectrum. The experimentally estimated ADEs of all bisulfate clusters, along with their vertical detachment energies (VDEs), measured from the rising onset peak maxima, are listed in Table 1.

To better understand the experimentally observed spectra and obtain insights into the first nucleation step of atmospheric aerosols, we conducted structural analysis using replica exchange molecular dynamics (REMD) simulations[52] and quantum chemical calculations.[53] (See the Supporting Information for the details of REMD and DFT methods.)

Table 1. Experimentally Measured and Theoretically Calculated Adiabatic (ADE) and Vertical Detachment Energy (VDE) for $HSO_4^-(Sol)_n$ (Sol = SUA, H_2O, and H_2SO_4) (n = 0−2) (in eV)

		ADE				VDE		
			$(isomer)^b$	calc.^{c}			$(isomer)^b$ calc.^{c}	
		expt.^{a}		B3LYP	M06-2X	expt.^{a}	B3LYP	M06-2X
HSO_4^-	X	4.75(10)		4.61	5.00	5.0(1)	4.86	5.36
	A	5.4(1)				5.68(10)		
	B	~5.8				6.22(10)		
	C	7.18(2)				7.28 (2)		
	freq. (cm^{-1})	800(40)		821.6^d				
$HSO_4^-(SUA)_1$	X	6.45(10)		5.87	6.27	6.78(10)	6.23	7.19
$HSO_4^-(H_2SO_4)_1$	X	6.55(10)		5.96	6.42	6.8(1)	6.50	7.20
$HSO_4^-(H_2O)_1$	X	5.35(10)	A	4.68	5.13	5.6(1)	5.39	5.90
			B	5.07	5.47		5.46	6.00
$HSO_4^-(SUA)_2$	X′	~6.6	A	5.78	6.11		6.59	7.71
	X	~7.1	B	6.26	7.15		6.51	7.65
$HSO_4^-(H_2SO_4)_2$	X′	~7.2	A	6.53	6.93		7.25	8.05
	X	~7.5	B	6.90	7.37		7.41	8.44
$HSO_4^-(H_2O)_2$	X	5.55(10)	B_1	5.10	5.57	5.8(1)	5.86	6.44
			A_1	4.79	5.20		5.57	6.11

^{a}Numbers in parentheses represent experimental uncertainty in last digits. ^{b}Optimized structures at B3LYP/6-311++G(3df,3pd) level of theory (Figure 2). ^{c}B3LYP/6-311++G(3df,3pd) level of theory. The ADEs and VDEs calculated at the M06-2X/aug-cc-PVT(+d)Z//B3LYP/6-311++G(3df,3pd) level of theory are also listed. All ADEs are corrected with zero-point vibrational energy differences. For $HSO_4^-(H_2O)_{1,2}$, $HSO_4^-(H_2SO_4)_{1,2}$, and $HSO_4^-(SUA)_1$, we also performed single-point energy calculations at the MP2//B3LYP/6-311++G(3df,3pd) level. See the Supporting Information for the MP2 values. ^{d}Listed theoretical vibrational frequency is after 0.970 scaling factor.

The potential energy surfaces of the clusters were first explored using REMD simulations using the semiempirical RM1 Hamiltonian.[54] The low-lying isomers (within 10 kcal/mol) obtained from the REMD simulations were further optimized using the B3LYP functional[55] with Pople's basis set 6-311++G(3df, 3pd),[56] followed by single-point energy calculations using both MP2[57] and DFT (M06-2X)[58] methods. The validity and accuracy of the theoretical methods were confirmed by comparison of the calculated geometries of H_2O, HSO_4^-, H_2SO_4, SUA, and SUA$^-$ (SUA$^-$ represents the deprotonated succinic acid anion) with the available experimental values and previous calculations. (See the Supporting Information, Figure S1 and Table S1.)

The most stable structures along with the low-lying isomers that provide good agreement with the EBE measurements for $HSO_4^-(Sol)_n$ (Sol = SUA, H_2O, and H_2SO_4) are shown in Figure 2 (additional isomers and the corresponding neutrals are shown in Figure S2 in the Supporting Information.) We present only our HSO_4^- results for comparison because this system has been studied thoroughly by Wang et al.[49] and others.[59] The calculated geometric structures, vibrational frequencies, as well as the ADE and VDE (X) (see Table 1 and Table S1 in the Supporting Information) of HSO_4^- are in excellent agreement with the experimental values.

There are two intermolecular H bonds between HSO_4^- and SUA and one intramolecular H bond in SUA in our optimized most stable structure of $HSO_4^-(SUA)_1$. As shown in Figure 2, the O···H···O contact distances are 2.558 and 2.617 Å for the two intermolecular H bonds between SUA and HSO_4^- and 2.593 Å for the intramolecular H bond of SUA. Therefore, all three H bonds correspond to strong H bonds.[60] The ADE and VDE calculated with the M06-2X functional are 6.27 and 7.19 eV, in good agreement with the experimental data and significantly larger than the corresponding values measured for free HSO_4^- (Table 1). This stabilization is due to the formation of multiple strong H bonds in the cluster.

The optimized structure of $HSO_4^-(H_2SO_4)_1$ possesses three intermolecular H bonds (Figure 2). Such structure has been identified in $HSO_4^-(H_2SO_4)(H_2O)_n$ by Froyd and Lovejoy.[34] Also, in this case, the calculated ADE and VDE are in good agreement with the experimental values. Other isomers with two H bonds all turned out to be energetically very high (>5 kcal/mol) (Figure S2 in the Supporting Information).

Two nearly isoenergetic isomers of $HSO_4^-(H_2O)_1$ have been found (Figure 2). In isomer A, the H_2O molecule acts as double donor and single acceptor in forming three H bonds, whereas in isomer B, the single H_2O molecule interacts with bisulfate via bifurcated H bonds. All H bonds in $HSO_4^-(H_2O)_1$ are not optimal due to the constrained O−H···O angles that are appreciably different from the ideal value of 180°. The comparison between the measured and calculated ADEs and VDEs suggests that both isomers A and B are present in the experiments. A similar conclusion has been drawn in an IRMPD study of $HSO_4^-(H_2O)_n$ by Yacovitch et al.[29]

The amount of EBE increase in $HSO_4^-(Sol)_1$ relative to that of HSO_4^- obtained from the experiments for Sol = water, sulfuric acid, and SUA agrees with the calculated ion−solvent binding energy reasonably, that is, ca. 11 (0.48 eV), 43 (1.86 eV), and 32 kcal/mol (1.39 eV), respectively (vide infra and Table S5 in the Supporting Information), and is consistent with the amount of electron transfer from HSO_4^- core ion to each solvent molecule, that is, 0.02|e| (water), 0.16|e| (sulfuric acid), and 0.31|e| (SUA) upon forming complexes (see Figure S3 in the Supporting Information for NBO charge analysis). It is also interesting to note there is proton transfer from SUA molecule (with the O−H bond length increasing from 0.969 Å in free SUA to 1.529 Å in the complex, see Figure 2 and Figure S1 in the Supporting Information) to bisulfate ion upon forming cluster. The bond length of the newly formed (S)O−H is 1.030 Å, similar to the other one of 1.012 Å, and both are just slightly longer than that found in free sulfuric acid (0.967 Å). Proton transfer results in a very strong H bond that can be understood
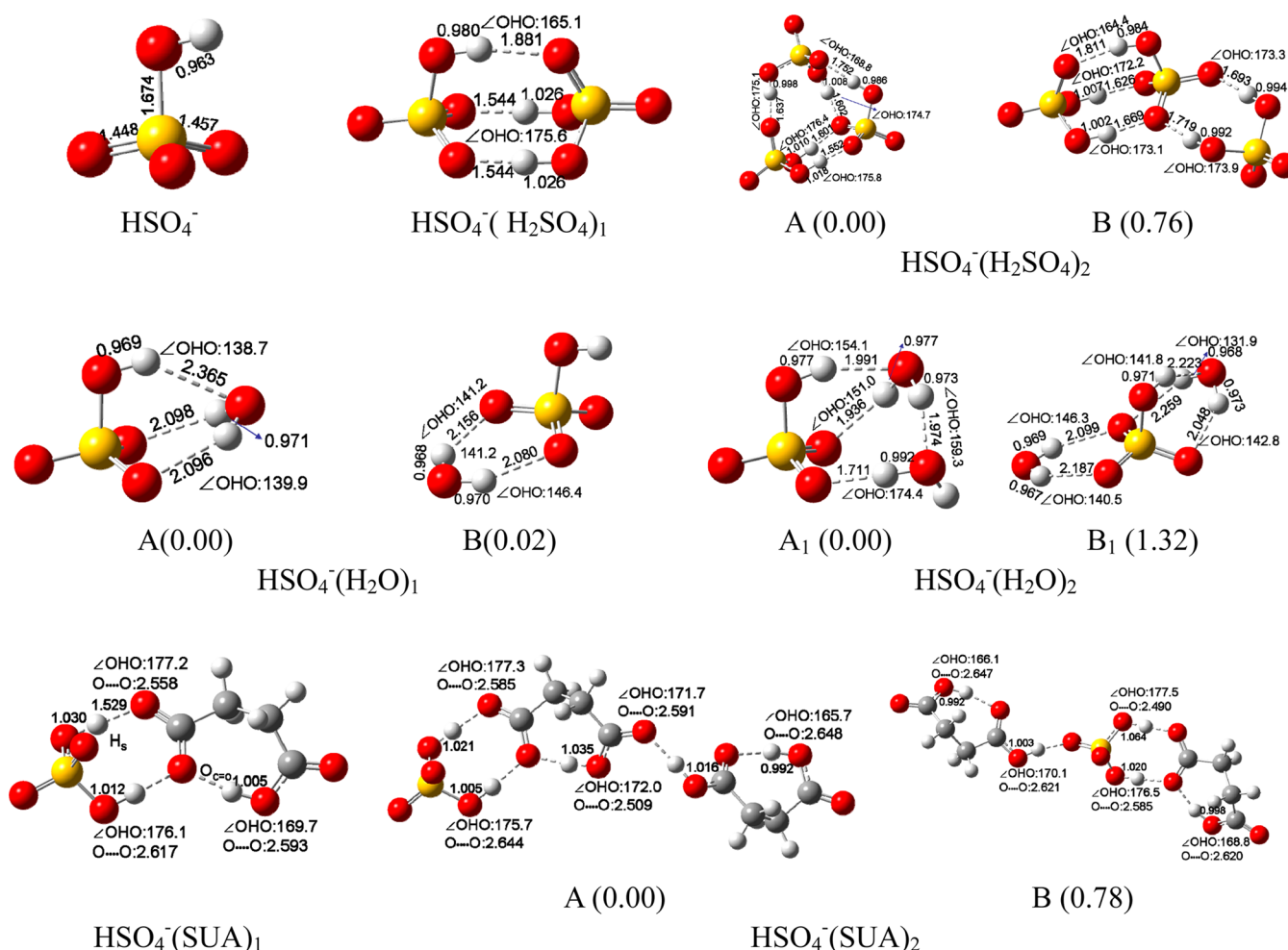
Figure 2. Most stable structures and low-lying isomers that show good agreement with the experiments of $HSO_4^-(Sol)_{0-2}$ (Sol = SUA, H_2SO_4, and H_2O) at the B3LYP/6-311++G(3df, 3pd) level. Selected bond lengths (Å), bond angles (deg), and relative energies (kcal/mol) are indicated.

by considering that the proton affinity (PA) of HSO_4^- (311.1/306.4 ± 3.1 kcal/mol)[16] does not differ much to that of SUA^- (322.8 kcal/mol).[16] A similar proton transfer mechanism has been observed previously by Ehn et al.[16] in $HSO_4^- \cdot$(malonic acid). The complexation also leads to a stronger intramolecular H bond (d(O···H···O) from 2.754 to 2.593 Å) of SUA, which can be attributed to the increased negative electron density on $O_{c=o}$ (from $-0.643|e|$ in SUA to $-0.795|e|$ in the cluster) (see Figure S3 in the Supporting Information for NBO charge analysis) due to proton transfer. Simultaneously, the charge of the shared transferred H_s slightly increases from $0.498|e|$ to $0.512|e|$. Therefore, this cluster can effectively be written as $(HSO_4^-)(H^+)(SUA^-)$ or $H_2SO_4(SUA^-)$ instead of $HSO_4^-(SUA)$. In contrast, there is no proton transfer occurred in $HSO_4^-(H_2O)_1$ because the PA of OH^- (390.7 kcal/mol)[61] is significantly larger than that of bisulfate.

Several low-lying isomers (within 4 kcal/mol at the B3LYP/6-311++G (3df, 3pd) level of theory) have been identified for $HSO_4^-(SUA)_2$ (Figure S2 in the Supporting Information), among which the two most stable structures are shown in Figure 2. Structure A has a linear configuration with HSO_4^- staying on one side and two SUA molecules connected by one strong intermolecular H bond (d(O···H···O)=2.591 Å). This configuration is similar to the structure of $(C_2H_2O_4)_2(HSO_4^-)$ obtained by Xu et al.[37] Compared with $HSO_4^-(SUA)_1$, it appears that proton transfer from SUA to HSO_4^- is more

significant. This can be attributed to the formation of the hydrogen bond between the two acid molecules that decreases the PA of the carboxylic acid group. As a consequence, this structure should probably be written as $(H_2SO_4)(SUA^-)$-(SUA). Isomer B also displays a linear structure, with HSO_4^- now lying between two SUA molecules. A similar structure has been predicted for $(H_2SO_4)($pinonic acid$)_2$ by Zhao et al.[38] and has been shown to enable further growth of the cluster by addition of other nucleated species on both sides. The computed M06-2X ADEs for A (6.11 eV) and B (7.15 eV) fit well with the experimental features of X′ (6.6 eV) and X (7.1 eV).

Six minima have been obtained for $HSO_4^-(H_2SO_4)_2$ (Figure S2 in the Supporting Information), several of which are also reported by Herb et al.[62] and by Froyd and Lovejoy[34] (in monohydrated clusters). The two most stable structures are isomer A, where each H_2SO_4 molecule interacts with bisulfate via two H bonds and connects with each other via one H bond, and structure B, where one H_2SO_4 associates with bisulfate via three H bonds as in the case for $HSO_4^-(H_2SO_4)_1$, whereas the other H_2SO_4 solvates the empty side of bisulfate. The M06-2X ADE is ca. 7 eV for A and ca. 7.4 eV for B, in good agreement with the experimental X′ (7.2 eV) and X (7.5 eV) features.

Up to 12 isomers for $HSO_4^-(H_2O)_2$ are identified (Figure S2 in the Supporting Information), with some of them already being reported in the literature.[29,35,50,63] The most stable

clusters are isomer A_1, which can be viewed as a water dimer (connected by one H bond) interacting with the anion core, and isomer B_1, in which each H_2O molecule interacts with only one side of HSO_4^-. Again the calculated M06-2X ADEs for both isomers fit the observed spectrum well, suggesting that both isomers likely exist under the experimental conditions, which supports the observations of Yacovitch et al. derived from the IRMPD experiments.[29]

To further understand the roles of organic diacids in aerosol nucleation, we calculated the thermochemical parameters (e.g., binding energy, enthalpy, entropy, and Gibbs free energy, Table S5 in the Supporting Information) for the complex formation at 1 atm and 298 K for the most stable isomers shown in Figure 2. Our calculations show very large binding energies of ∼32 kcal/mol for $HSO_4^-(SUA)_1$ and ∼50 kcal/mol for $HSO_4^-(SUA)_2$. These values are much larger than that of $HSO_4^-(H_2O)_1$ (∼11 kcal/mol) and $HSO_4^-(H_2O)_2$ (∼21 kcal/mol), in accord with the conclusions derived from the EBE increase that SUA can induce a larger stabilization of the bisulfate ion than H_2O. The Gibbs free energy changes (ΔG) for bisulfate associated with one and two SUAs are calculated to be ca. −20 and −27 kcal/mol, respectively, much larger than the corresponding values, ca. −2.5 and −4.7 kcal/mol, for one and two water molecules. The large binding energies and negative Gibbs free energy changes for bisulfate-SUA clusters indicate that these complexes are very stable, thermodynamically favorable to form, and can survive for long times under atmospheric conditions. Consequently they may contribute to reducing nucleation barriers[17,64] and facilitate further growth into larger particles. Considering the abundance of organic dicarboxylic acid in the atmosphere,[18,20] it is likely that organic dicarboxylic acids will play critical roles in stabilizing gaseous bisulfate ion by forming highly stable complex and promoting the aerosol nucleation.

In the atmosphere, most of molecular clusters involved in the nucleation process are charge neutral. It is interesting to note that Zhang and coworkers have recently reported the binding energies of neutral sulfuric acid with H_2O, H_2SO_4, and SUA molecule to be ca. 9.1, 13.1, and 12.8 kcal/mol and the Gibbs free energy changes to be ca. −2.7, −5.7, −4.9 kcal/mol, respectively.[40] Although the absolute thermodynamic quantity is found to be much smaller for the neutral species, the trend across the three solvent molecules studied here is in good accord with that for the charged $HSO_4^-(Sol)_1$ species. This agreement suggests that the conclusions drawn from the current study most likely can also be applied to the neutral case. It is worth pointing out that besides thermodynamic perspective, which is the focus of the current study, kinetic factors are also expected to play important roles in aerosol nucleation processes.[8,23]

In summary, the anionic complex clusters formed by key atmospheric nucleation species, such as sulfuric acid/bisulfate ion and a common organic diacid (succinic acid), have been successfully produced by ESI, and their energetics and structures have been investigated by using low-temperature PES combined with theoretical calculations. The observed PE spectra show that these complexes possess very high EBEs, with a huge EBE increase, by 1.7 eV for the first SUA relative to EBE of HSO_4^-, compared with the 0.6 eV EBE increase measured for the first H_2O. Replica exchange simulations and electronic structure calculations identify three strong H bonds in $HSO_4^-(SUA)_1$, which serve as the driving force for the complex formation and account for the high stability of the complex. Comparison with other prenucleation species reveals

that the formation of $HSO_4^-(SUA)_n$ anionic complexes is thermodynamically much more favorable than $HSO_4^-(H_2O)_n$. Given the abundance of organic diacids in the atmosphere, their complexion with sulfuric acid/bisulfate ion can significantly reduce the nucleation barrier, which will facilitate further growth of the new aerosol particles.

■ ASSOCIATED CONTENT

ⓢ Supporting Information

Experimental and theoretical sections, optimized structures of monomer species, additional low-lying isomers of anion and neutral clusters, calculated ADEs and VDEs of all isomers, thermodynamic parameters for each complex formation, and NBO analysis. This material is available free of charge via the Internet at http://pubs.acs.org.

■ AUTHOR INFORMATION

Corresponding Author
*E-mail: xuebin.wang@pnnl.gov.

Present Address
‖Visiting students via PNNL alternate sponsored fellowship. Permanent address for J.Z.: State Key Laboratory of Precision Spectroscopy, East China Normal University, Shanghai 200062, China.

Notes
The authors declare no competing financial interest.

■ ACKNOWLEDGMENTS

■ REFERENCES

(1) Kulmala, M. How Particles Nucleate and Grow. *Science* **2003**, *302*, 1000−1001.

(2) Charlson, R. J.; Schwartz, S. E.; Hales, J. M.; Cess, R. D.; Coakley, J. A.; Hansen, J. E.; Hofmann, D. J. Climate Forcing by Anthropogenic Aerosols. *Science* **1992**, *255*, 423−430.

(3) Power, H. C. The Geography and Climatology of Aerosols. *Pro. Phys. Geography* **2003**, *27*, 502−547.

(4) Dockery, D. W.; Schwartz, J.; Spengler, J. D. Air Pollution and Daily Mortality: Associations with Particulates and Acid Aerosols. *Environ. Res.* **1992**, *59*, 362−373.

(5) Dockery, D. W.; Pope, C. A. Acute Respiratory Effects of Particulate Air Pollution. *Annu. Rev. Public Health* **1994**, *15*, 107−132.

(6) Saxon, A.; Diaz-Sanchez, D. Air Pollution and Allergy: You Are What You Breathe. *Nat. Immunol.* **2005**, *6*, 223−226.

(7) Kittelson, D. B.; Watts, W. F.; Johnson, J. P. Nanoparticle Emissions on Minnesota Highways. *Atmos. Environ.* **2004**, *38*, 9−19.

(8) Zhang, R. Y.; Khalizov, A.; Wang, L.; Hu, M.; Xu, W. Nucleation and Growth of Nanoparticles in the Atmosphere. *Chem. Rev.* **2012**, *112*, 1957−2011.

(9) Kathmann, S. M.; Schenter, G. K.; Garrett, B. C.; Chen, B.; Siepmann, J. I. Thermodynamics and Kinetics of Nanoclusters Controlling Gas-to-Particle Nucleation. *J. Phys. Chem. C* **2009**, *113*, 10354−10370.

(10) Sipilä, M.; Berndt, T.; Petäjä, T.; Brus, D.; Vanhanen, J.; Stratmann, F.; Patokoski, J.; Mauldin, R. L. I.; Hyvärinen, A.-P.; Lihavainen, H.; Kulmala, M. The Role of Sulfuric Acid in Atmospheric Nucleation. *Science* **2010**, *327*, 1243−1246.

(11) Hamill, P.; Turco, R. P.; Kiang, C. S.; Toon, O. B.; Whitten, R. C. An Analysis of Various Nucleation Mechanisms for Sulfate Particles in the Stratosphere. *J. Aerosol Sci.* **1982**, *13*, 561−585.

(12) Kulmala, M.; Korhonen, P.; Napari, I.; Karlsson, A.; Berresheim, H.; O'Dowd, C. D. Aerosol Formation During PARFORCE: Ternary Nucleation of H_2SO_4, NH_3, and H_2O. *J. Geophys. Res.* **2002**, *107*, 8111.

(13) Napari, I.; Noppel, M.; Vehkamäki, H.; Kulmala, M. Parametrization of Ternary Nucleation Rates for H_2SO_4-NH_3-H_2O Vapors. *J. Geophys. Res.* **2002**, *107*, 4381.

(14) Loukonen, V.; Kurtén, T.; Ortega, I. K.; Vehkamäki, H.; Pádua, A. A. H.; Sellegri, K.; Kulmala, M. Enhancing Effect of Dimethylamine in Sulfuric Acid Nucleation in the Presence of Water − a Computational Study. *Atmos. Chem. Phys.* **2010**, *10*, 4961−4974.

(15) DePalma, J. W.; Bzdek, B. R.; Doren, D. J.; Johnston, M. V. Structure and Energetics of Nanometer Size Clusters of Sulfuric Acid with Ammonia and Dimethylamine. *J. Phys. Chem. A* **2012**, *116*, 1030−1040.

(16) Ehn, M.; Junninen, H.; Petäjä, T.; Kurtén, T.; Kerminen, V. M.; Schobesberger, S.; Manninen, H. E.; Ortega, I. K.; Vehkamäki, H.; Kulmala, M.; Worsnop, D. R. Composition and Temporal Behavior of Ambient Ions in the Boreal Forest. *Atmos. Chem. Phys.* **2010**, *10*, 8513−8530.

(17) Yu, F.; Turco, R. P. Ultrafine Aerosol Formation via Ion-Mediated Nucleation. *Geophys. Res. Lett.* **2000**, *27*, 883−886.

(18) Prenni, A. J.; DeMott, P. J.; Kreidenweis, S. M.; Sherman, D. E. The Effects of Low Molecular Weight Dicarboxylic Acids on Cloud Formation. *J. Phys. Chem. A* **2001**, *105*, 11240−11248.

(19) Marti, J. J.; Weber, R. J.; McMurry, P. H.; Eisele, F.; Tanner, D.; Jefferson, A. New Particle Formation at a Remote Continental Site: Assessing the Contributions of SO_2 and Organic Precursors. *J. Geophys. Res.* **1997**, *102*, 6331−6339.

(20) Limbeck, A.; Puxbaum, H.; Otter, L.; Scholes, M. C. Semivolatile Behavior of Dicarboxylic Acids and Other Polar Organic Species at a Rural Background Site (Nylsvley, RSA). *Atmos. Environ.* **2001**, *35*, 1853−1862.

(21) Hõrrak, U.; Salm, J.; Tammet, H. Bursts of Intermediate Ions in Atmospheric Air. *J. Geophys. Res.* **1998**, *103*, 13909−13915.

(22) Keesee, R. G.; Castleman, A. W. J. Ions and Cluster Ions: Experimental Studies and Atmospheric Observations. *J. Geophys. Res.* **1985**, *90*, 5885−5890.

(23) Zhang, R. Y.; Suh, I.; Zhao, J.; Zhang, D.; Fortner, E. C. ; Tie, X.; Molina, L. T.; Molina, M. J. Atmospheric New Particle Formation Enhanced by Organic Acids. *Science* **2004**, *304*, 1487−1490.

(24) Zhang, R.; Wang, L.; Khalizov, A. F.; Zhao, J.; Zheng, J.; McGraw, R. L.; Molinac, L. T. Formation of Nanoparticles of Blue Haze Enhanced by Anthropogenic Pollution. *Proc. Natl. Acad. Sci. U.S.A.* **2009**, *106*, 17650−17654.

(25) Wang, L.; Xu, W.; Khalizov, A. F.; Zheng, J.; Qiu, C.; Zhang, R. Y. Laboratory Investigation on the Role of Organics in Atmospheric Nanoparticle Growth. *J. Phys. Chem. A* **2011**, *115*, 8940−8947.

(26) Lal, V.; Khalizov, A. F.; Lin, Y.; Galvan, M. D.; Connell, B. T.; Zhang, R. Y. Heterogeneous Reactions of Epoxides in Acidic Media. *J. Phys. Chem. A* **2012**, *116*, 6078−6090.

(27) Peckhaus, A.; Grass, S.; Treuel, L.; Zellner, R. Deliquescence and Efflorescence Behavior of Ternary Inorganic/Organic/Water Aerosol Particles. *J. Phys. Chem. A* **2012**, *116*, 6199−6210.

(28) Wang, L.; Khalizov, A. F.; Zheng, J.; Xu, W.; Ma, Y.; Lal, V.; Zhang, R. Y. Atmospheric Nanoparticles Formed from Heterogeneous Reactions of Organics. *Nat. Geosci.* **2010**, *3*, 238−242.

(29) Yacovitch, T. I.; Wende, T.; Jiang, L.; Heine, N.; Meijer, G.; Neumark, D. M.; Asmis, K. R. Infrared Spectroscopy of Hydrated Bisulfate Anion Clusters: $HSO_4^-(H_2O)_{1-16}$. *J. Phys. Chem. Lett.* **2011**, *2*, 2135−2140.

(30) Yacovitch, T. I.; Heine, N.; Brieger, C.; Wende, T.; Hock, C.; Neumark, D. M.; Asmis, K. R. Communication: Vibrational Spectroscopy of Atmospherically Relevant Acid Cluster Anions: Bisulfate versus Nitrate Core Structures. *J. Chem. Phys.* **2012**, *136*, 241102.

(31) Zatula, A. S.; Andersson, P. U.; Ryding, M. J.; Uggerud, E. Proton Mobility and Stability of Water Clusters Containing the Bisulfate Anion, $HSO_4^-(H_2O)_n$. *Phys. Chem. Chem. Phys.* **2011**, *13*, 13287−13294.

(32) Lovejoy, E. R.; Curtius, J. Cluster Ion Thermal Decomposition (II): Master Equation Modeling in the Low-Pressure Limit and Fall-Off Regions. Bond Energies for $HSO_4^-(H_2SO_4)_x(HNO_3)_y$. *J. Phys. Chem. A* **2001**, *105*.

(33) Curtius, J.; Froyd, K. D.; Lovejoy, E. R. Cluster Ion Thermal Decomposition (I): Experimental Kinetics Study and ab Initio Calculations for $HSO_4(H_2SO_4)_x(HNO_3)_y$. *J. Phys. Chem. A* **2001**, *105*, 10867−10873.

(34) Froyd, K. D.; Lovejoy, E. R. Experimental Thermodynamics of Cluster Ions Composed of H_2SO_4 and H_2O. 2. Measurements and ab Initio Structures of Negative Ions. *J. Phys. Chem. A* **2003**, *107*, 9812−9824.

(35) Husar, D. E.; Temelso, B.; Ashworth, A. L.; Shields, G. C. Hydration of the Bisulfate Ion: Atmospheric Implications. *J. Phys. Chem. A* **2012**, *116*, 5151−5163.

(36) Temelso, B.; Morrell, T. E.; Shields, R. M.; Allodi, M. A.; Wood, E. K.; Kirschner, K. N.; Castonguay, T. C.; Archer, K. A.; Shields, G. C. Quantum Mechanical Study of Sulfuric Acid Hydration: Atmospheric Implications. *J. Phys. Chem. A* **2012**, *116*, 2209−2224.

(37) Xu, Y.; Nadykto, A. B.; Yu, F.; Jiang, L.; Wang, W. Formation and Properties of Hydrogen-Bonded Complexes of Common Organic Oxalic Acid with Atmospheric Nucleation Precursors. *J. Mol. Struct.: THEOCHEM* **2010**, *951*, 28−33.

(38) Zhao, J.; Khalizov, A.; Zhang, R. Y.; McGraw, R. Hydrogen-Bonding Interaction in Molecular Complexes and Clusters of Aerosol Nucleation Precursors. *J. Phys. Chem. A* **2009**, *113*, 680−689.

(39) Xu, Y.; Nadykto, A. B.; Yu, F.; Herb, J.; Wang, W. Interaction between Common Organic Acids and Trace Nucleation Species in the Earth's Atmosphere. *J. Phys. Chem. A* **2010**, *114*, 387−396.

(40) Xu, W.; Zhang, R. Y. Theoretical Investigation of Interaction of Dicarboxylic Acids with Common Aerosol Nucleation Precursors. *J. Phys. Chem. A* **2012**, *116*, 4539−4550.

(41) Nadykto, A. B.; Yu, F. Strong Hydrogen Bonding between Atmospheric Nucleation Precursors and Common Organics. *Chem. Phys. Lett.* **2007**, *435*, 14−18.

(42) Weber, K. H.; Morales, F. J.; Tao, F.-M. Theoretical Study on the Structure and Stabilities of Molecular Clusters of Oxalic Acid with Water. *J. Phys. Chem. A* **2012**, *116*, 11601−11617.

(43) Zhang, R. Y. Getting to the Critical Nucleus of Aerosol Formation. *Science* **2010**, *328*, 1366−1367.

(44) Wang, X.-B.; Wang, L.-S. Development of a Low-Temperature Photoelectron Spectroscopy Instrument Using an Electrospray Ion Source and a Cryogenically Controlled Ion Trap. *Rev. Sci. Instrum.* **2008**, *79*, 073108.

(45) Wang, X. B.; Wang, L. S. Bulk-Like Features in the Photoemission Spectra of Hydrated Doubly Charged Anion Clusters. *Science* **2001**, *294*, 1322−1325.

(46) Murdachaew, G.; Valiev, M.; Kathmann, S. M.; Wang, X.-B. Study of Ion Specific Interactions of Alkali Cations with Dicarboxylate Dianions. *J. Phys. Chem. A* **2012**, *116*, 2055−2061.

(47) Minofar, B.; Mucha, M.; Jungwirth, P.; Yang, X.; Fu, Y.-J.; Wang, X.-B.; Wang, L.-S. Bulk versus Interfacial Aqueous Solvation of Dicarboxylate Dianions. *J. Am. Chem. Soc.* **2004**, *126*, 11691−11698.

(48) Woo, H.-K.; Wang, X.-B.; Lau, K.-C.; Wang, L.-S. Low-temperature Photoelectron Spectroscopy of Aliphatic Dicarboxylate Monoanions, $HO_2C(CH_2)_nCO_2^-$ (n = 1−10): Hydrogen Bond Induced Cyclization and Strain Energies. *J. Phys. Chem. A* **2006**, *110*, 7801−7805.

(49) Wang, X.-B.; Nicholas, J. B.; Wang, L.-S. Photoelectron Spectroscopy and Theoretical Calculations of SO_4^- and HSO_4^-: Confirmation of High Electron Affinities of SO_4 and HSO_4. *J. Phys. Chem. A* **2000**, *104*, 504−508.

(50) Kurtén, T.; Noppel, M.; Vehkamäki, H.; Salonen, M.; Kulmala, M. Quantum Chemical Studies of Hydrate Formation of H_2SO_4 and HSO_4^-. *Boreal Environ. Res.* **2007**, *12*, 431−453.

(51) Eisele, F. L.; Hanson, D. R. First Measurement of Prenucleation Molecular Clusters. *J. Phys. Chem. A* **2000**, *104*, 830−836.

(52) Yuji, S.; Okamoto, Y. Replica-Exchange Molecular Dynamics Method for Protein Folding. *Chem. Phys. Lett.* **1999**, *314*, 141−151.

(53) Frisch, M. J.; Trucks, G. W.; Schlegel, H. B. *Gaussian 09*; Gaussian, Inc: Wallingford, CT, 2009.

(54) Rocha, G. B.; Freire, R. O.; Simas, A. M.; Stewart, J. J. P. RM1: A Reparameterization of AM1 for H, C, N, O, P, S, F, Cl, Br, and I. *J. Comput. Chem.* **2006**, *27*, 1101−1111.

(55) (a) Becke, A. D. Density Functional Thermochemistry. III. The Role of Exact Exchange. *J. Chem. Phys.* **1993**, *98*, 5648−5652. (b) Lee, C.; Yang, W.; Parr, R. G. Development of the Colle-Salvetti Correlation-Energy Formula into a Functional of the Electron Density. *Phys. Rev. B* **1988**, *37*, 785−789.

(56) Krishnan, R.; Binkley, J. S.; Seeger, R.; Pople, J. A. Self-Consistent Molecular Orbital Methods. XX. a Basis Set for Correlated Wave Functions. *J. Chem. Phys.* **1980**, *72*, 650−654.

(57) Head-Gordon, M.; Pople, J. A.; Frisch, M. J. MP2 Energy Evaluation by Direct Methods. *Chem. Phys. Lett.* **1988**, *153*, 503−506.

(58) Zhao, Y.; Truhlar, D. G. Density Functionals with Broad Applicability in Chemistry. *Acc. Chem. Res.* **2008**, *41*, 157−167.

(59) Vchirawongkwin, V.; Kritayakornupong, C.; Rode, B. M. Structural and Dynamical Properties and Vibrational Spectra of Bisulfate Ion in Water: A Study by Ab Initio Quantum Mechanical Charge Field Molecular Dynamics. *J. Phys. Chem. B* **2010**, *114*, 11561−11569.

(60) Gilli, P.; Bertolasi, V.; Ferretti, V.; Gilli, G. Covalent Nature of the Strong Homonuclear Hydrogen Bond. Study of the O⋯H⋯O System by Crystal Structure Correlation Methods. *J. Am. Chem. Soc.* **1994**, *116*, 909−915.

(61) NIST Chemistry WebBook. http://webbook.nist.gov (accessed February 8, 2013).

(62) Herb, J.; Xu, Y.; Yu, F.; Nadykto, A. B. Large Hydrogen-Bonded Pre-nucleation $(HSO_4^-)(H_2SO_4)_m(H_2O)_k$ and $(HSO_4^-)(NH_3)$-$(H_2SO_4)_m(H_2O)_k$ Clusters in the Earth's Atmosphere. *J. Phys. Chem. A* **2013**, *117*, 133−152.

(63) Nadykto, A. B.; Yu, F.; Herb, J. Theoretical Analysis of the Gas-Phase Hydration of Common Atmospheric Pre-Nucleation and $(H_3O^+)(H_2SO_4)(H_2O)_n$ Cluster Ions. *Chem. Phys.* **2009**, *360*, 67−73.

(64) Curtius, J.; Lovejoy, E. R.; Froyd, K. D. Atmospheric Ion-Induced Aerosol Nucleation. *Space Sci. Rev.* **2006**, *125*, 159−167.